

The Excitation Energy Dependence of the Total Kinetic Energy Release in $^{235}\text{U}(\text{n},\text{f})$

R. Yanez, L. Yao, J. King, and W. Loveland

Department of Chemistry, Oregon State University, Corvallis, OR, 97331.

F. Tovesson and N. Fotiades

Los Alamos National Laboratory, Los Alamos, NM 87545

(Dated: March 19, 2014)

Abstract

The total kinetic energy release in the neutron induced fission of ^{235}U was measured (using white spectrum neutrons from LANSCE) for neutron energies from $E_n = 3.2$ to 50 MeV. In this energy range the average post-neutron total kinetic energy release drops from 167.4 ± 0.7 to 162.1 ± 0.8 MeV, exhibiting a local dip near the second chance fission threshold. The values and the slope of the TKE vs. E_n agree with previous measurements but do disagree (in magnitude) with systematics. The variances of the TKE distributions are larger than expected and apart from structure near the second chance fission threshold, are invariant for the neutron energy range from 11 to 50 MeV. We also report the dependence of the total excitation energy in fission, TXE, on neutron energy.

PACS numbers: 25.70.Jj, 25.85.-w, 25.60.Pj, 25.70.-z

I. INTRODUCTION

Most of the energy released in the nuclear fission process appears in the kinetic energy of the fission fragments. A first order estimate of the magnitude of the total kinetic energy release is that of the Coulomb energy of the fragments at scission, i.e.,

$$V_{Coul} = \frac{Z_1 Z_2 e^2}{r_1 + r_2} \quad (1)$$

where Z_n , r_n are the atomic numbers and radii of fragments 1 and 2. Recognizing that the fragments are deformed at scission, one can re-write equation 1 as

$$TKE = \frac{Z_1 Z_2 e^2}{1.9(A_1^{1/3} + A_2^{1/3})} \quad (2)$$

where the coefficient 1.9 (instead of the usual 1.2 - 1.3) represents the fragment deformation. For symmetric fission, $Z_1=Z_2=Z/2$ and $A_1=A_2=A/2$, then we have

$$TKE = (0.119) \frac{Z^2}{A^{1/3}} MeV \quad (3)$$

Trajectory calculations [1] for alpha particle emission in fission have shown that the fission fragments are in motion at scission with a pre-scission kinetic energy of 7.3 MeV and an additive term representing this motion is needed. Thus we have the “Viola systematics” [2] that say

$$TKE = (0.1189 \pm 0.0011) \frac{Z^2}{A^{1/3}} + 7.3(\pm 1.5) MeV \quad (4)$$

The deformed scission point fragments will contract to their equilibrium deformations and the energy stored in deformation will be converted into internal excitation energy. Thus we can define a related quantity, the total excitation energy , TXE, in fission as

$$TXE = Q - TKE \quad (5)$$

where Q is the mass-energy release. One quickly realizes that these quantities depend on the mass split in fission which in turn, at low excitation energies, may reflect the fragment nuclear structure. The TXE is the starting point for calculations of the prompt neutron and gamma emission in fission, the yields of beta emitting fission fragments, reactor anti-neutrino spectra, etc. As such, it is a fundamental property of all fissioning systems and sadly not very well known.

As a practical matter, one needs to know the dependence of the TKE and TXE on neutron energy for the neutron induced fission of technologically important actinide fissioning systems like $^{233}\text{U}(\text{n},\text{f})$, $^{235}\text{U}(\text{n},\text{f})$, and $^{239}\text{Pu}(\text{n},\text{f})$. The first question we might pose is whether the TKE should depend on the excitation energy of the fissioning system. Does the energy brought in by an incident neutron in neutron induced fission appear in the fragment excitation energy or does it appear in the total kinetic energy? In a variety of experiments, one finds that increasing the excitation energy of the fissioning system does not lead to significant increases in the TKE of the fission fragments or changes in the fragment separation at scission. [3]. However, there may be more subtle effects that render this statement false in some circumstances. For example, we expect, on the basis of the Coulomb energy systematics given above, that the TKE will be proportional to changes in the fission mass splits which in turn can depend on the excitation energy.

For the technologically important reaction $^{235}\text{U}(\text{n},\text{f})$, Madland [4] summarizes the known data [5–7] with the following equations

$$\langle T_f^{tot} \rangle = (170.93 \pm 0.07) - (0.1544 \pm 0.02) E_n (\text{MeV}) \quad (6)$$

$$\langle T_p^{tot} \rangle = (169.13 \pm 0.07) - (0.2660 \pm 0.02) E_n (\text{MeV}) \quad (7)$$

where E_n is the energy of the incident neutron and T_f^{tot} and T_p^{tot} are the average total fission fragment kinetic energy (before neutron emission) and the average fission product kinetic energy after neutron emission, respectively. These quantities are related by the relation

$$\langle T_p^{tot}(E_n) \rangle = \langle T_f^{tot}(E_n) \rangle \left[1 - \frac{\overline{\nu_p}(E_n)}{2A} \left(\frac{\langle A_H \rangle}{\langle A_L \rangle} + \frac{\langle A_L \rangle}{\langle A_H \rangle} \right) \right] \quad (8)$$

These data show a modest decrease in TKE with increasing excitation energy for the neutron energy interval $E_n = 1\text{--}9$ MeV. There is no clearly identified changes in the TKE values near the second chance fission threshold, a feature that is important in semi-empirical models of fission such as represented by the GEF code.[8]

In this paper, we report the results of measuring the total kinetic energy release in the neutron induced fission of ^{235}U for neutron energies $E_n = 3.2\text{--}50$ MeV. The method used for the measurement is the 2E method, i.e., measurement of the kinetic energies of the two coincident fission products using semiconductor detectors. The time of flight of the neutrons inducing fission was measured, allowing deduction of their energy. The details of the experiment are discussed in Section II while the experimental results and a comparison

of the results with various models and theories is made in Section III with conclusions being summarized in Section IV.

II. EXPERIMENTAL

This experiment was carried out at the Weapons Neutron Research Facility (WNR) at the Los Alamos Neutron Science Center (LANSCE) at the Los Alamos National Laboratory [9, 10]. “White spectrum” neutron beams were generated from an unmoderated tungsten spallation source using the 800 MeV proton beam from the LANSCE linac. The experiment was located on the 15R beam line (15°-right with respect to the proton beam). The calculated (MCNPX) “white spectrum ” at the target position is shown in figure 1. [11] The proton beam is pulsed allowing one to measure the time of flight (energy) of the neutrons arriving at the experimental area.

A schematic diagram of the experimental apparatus is shown in figure 2. The neutron beam was collimated to a 1 cm diameter at the entrance to the experimental area. At the entrance to the scattering chamber, the beam diameter was measured to be 1.3 cm. A fission ionization chamber [12] was used to continuously monitor the absolute neutron beam intensities. The ^{235}U target and the Si PIN diode fission detectors were housed in an evacuated, thin-walled aluminum scattering chamber. The scattering chamber was located ~ 3.1 m from the collimator, and ~ 11 m from the neutron beam dump. The center of the scattering chamber was located 16.46 m from the production target.

The ^{235}U target consisted of a deposit of $^{235}\text{UF}_4$ on a thin C backing. The thickness of the ^{235}U was $175.5 \mu\text{g } ^{235}\text{U}/\text{cm}^2$ while the backing thickness was $100 \mu\text{g}/\text{cm}^2$. The isotopic purity of the ^{235}U was 99.91 %. The target was tilted at 50° with respect to the incident beam.

Fission fragments were detected by two arrays of Si PIN photodiodes (Hamamatsu S3590-09) arranged on opposite sides of the beam. The area of the individual PIN diodes was 1 cm^2 . The distance of the detectors from the target varied with angle from 2.60 cm to 4.12 cm. The coincident detector pairs were at approximately 45, 60, 90, 115, and 135° . The alpha particle energy resolution of the diodes was 18 keV for the 5475 keV line of ^{241}Am .

The time of flight of each interacting neutron was measured using a timing pulse from a Si PIN diode and the accelerator RF signal. Absolute calibrations of this time scale

were obtained from the photofission peak in the fission spectra and the known flight path geometry.

The energy calibration of the fission detectors was done with a ^{252}Cf source. We have used the traditional Schmitt method [13]. Some have criticized this method especially for PIN diodes. However with our limited selection of detectors, we were unable to apply the methods of [14] to achieve a robust substitute for the Schmitt method.

The measured fragment energies have to be corrected for energy loss in the $^{235}\text{UF}_4$ deposit and the C backing foil. This correction was done by scaling the energy loss correction given by the Northcliffe-Schilling energy loss tables [15] to a measured mean energy loss of collimated beams of light and heavy ^{252}Cf fission fragments in $100\text{ }\mu\text{ g/cm}^2$ C foils. The scaling factor that was used was a linear function of mass using the average loss of the heavy and light fission fragments as anchor points. The correction factors at the anchor points were 1.24 and 1.45 for the heavy and light fragments, respectively. Similar factors were obtained if the SRIM code [16] was used to calculate dE/dx . These large deviation factors from measured to calculated fission fragment stopping powers have been observed in the past [17], and represent the largest systematical uncertainty in the determination of the kinetic energies.

III. RESULTS AND DISCUSSION

The measured average post-neutron emission fission product total kinetic energy release for the $^{235}\text{U}(n,f)$ reaction (Table 1) is shown in Figure 3 along with other data and predictions [18–20]. The evaluated post-neutron emission data from Madlund [4] are shown as a dashed line while the individual pre-neutron emission measurements of [7] are shown as points. The point at $E_n = 14$ MeV is the average of [18] and [20]. The slope of the measured TKE release (this work) is in rough agreement with the previous measurements [4] at lower energies. Also shown are the predictions of the GEF model [8]. GEF is a semi-empirical model of fission that provides a good description of fission observables using a modest number of adjustable parameters. The dashed line in Figure 1 is a semi-empirical equation ($\text{TKE} = 171.5 - 0.1E^*$ for $E^* > 9$ MeV) suggested by Tudora et al. [21]. Qualitatively the decrease in TKE with increasing neutron energy reflects the increase in symmetric fission (with its lower associated TKE release) with increasing excitation energy. This general dependence is reflected in the

GEF code predictions with the slope of our data set being similar to the predictions of the GEF model but with the absolute values of the TKE release being substantially less.

In Figure 4, we show some typical TKE distributions along with Gaussian representations of the data. In general, the TKE distributions appear to be Gaussian in shape. This is in contrast to previous studies [22, 23] which showed a sizable skewness in the distributions.

In Figure 5, we show the dependence of the measured values of the variance of the TKE distributions as a function of neutron energy along with the predictions of the GEF model of the same quantity. The measured variances are larger than expected. At low energies (near the second chance fission threshold) the observed variances show a dependence on neutron energy similar to that predicted by the GEF model, presumably reflecting the changes in variance with decreasing mass asymmetry. At higher energies (11-50 MeV) the variances are roughly constant with changes in neutron energy. Models [24] would suggest that most of the variance of the TKE distribution is due to fluctuations in the nascent fragment separation at scission. The constancy of the variances is puzzling.

Using the Q values predicted by the GEF code, one can make a related plot (Fig. 6) of the TXE values in the $^{235}\text{U}(\text{n},\text{f})$ reaction. The “bump” in the TXE at lower neutron energies is pronounced and the dependence of the TXE upon neutron energy agrees with the GEF predictions although the absolute values are larger.

IV. CONCLUSIONS

We conclude that : (a) For the first time, we have measured the TKE release and its variance for the technologically important $^{235}\text{U}(\text{n},\text{f})$ reaction over a large range of neutron energies (3.2 - 50 MeV). (b) The dependence of the TKE upon E_n seems to agree with semi-empirical models although the absolute value does not. (c) Understanding the variance and its energy dependence for the TKE distribution remains a challenge.

Acknowledgments

This work was supported in part by the Director, Office of Energy Research, Division of Nuclear Physics of the Office of High Energy and Nuclear Physics of the U.S. Department of Energy under Grant DE-FG06-97ER41026. One of us (WL) wishes to thank the [Department

of Energy's] Institute for Nuclear Theory at the University of Washington for its hospitality and the Department of Energy for partial support during the completion of this work. This work has benefited from the use of the Los Alamos Neutron Science Center at the Los Alamos National Laboratory. This facility is funded by the U. S. Department of Energy under DOE Contract No. DE-AC52-06NA25396.

-
- [1] M. Rajagopalan and T.D. Thomas, Phys. Rev. C **5**, 2064 (1972).
 - [2] V.E. Viola, K. Kwiatkowski, and M. Walker, Phys. Rev. C **31**, 1550 (1985).
 - [3] R. Vandenbosch and J.R. Huizenga, Nuclear Fission (Academic, New York, 1973)
 - [4] D.G. Madlund, Nucl. Phys. A **772**, 113 (2006)
 - [5] Ch. Straede, C. Budtz-Jorgensen, and H.H. Knitter, Nucl. Phys. A **462**, 85 (1987).
 - [6] J.W. Meadows and C. Budtz-Jorgensen, ANL/NDM-64, 1982
 - [7] R. Muller, A.A. Naqvi, F. Kappeler, and F. Dickman, Phys. Rev. C **29**, 885 (1984).
 - [8] <http://www.cenbg.in2p3.fr/-GEF->
 - [9] P. W. Lisowski, C. D. Bowman, G. J. Russell, and S. A. Wender, Nucl. Sci. Eng. **106**, 208 (1990).
 - [10] P. W. Lisowski and K. F. Schoenberg, Nucl. Instr. Meth. in Phys. Res. A **562**, 910 (2006).
 - [11] K. Baba et al., arXiv:1310.8593v1 [hep-ex] 31 Oct 2013
 - [12] S.A. Wender et al., Nucl. Instru. Meth. Phys. Res. A **336**, 226 (1993)
 - [13] H.W. Schmitt, W.E. Kiker, and C.W. Williams, Phys. Rev. B **4**, 837 (1965)
 - [14] S.I. Mulgin, V.N. Okolovich, and S.V. Zhudanov, Nucl. Instru. Meth, Phys. Res. A **388**, 254 (1997)
 - [15] L.C. Northcliffe and R.F. Schilling, At, Data and Nucl. Data Tables, **7**, 233 (1970)
 - [16] J.F. Ziegler, M.D. Ziegler b, J.P. Biersack, Nucl. Instr. Meth. Phys. Res. **B268**, 1818 (2010).
 - [17] G.N. Knyazheva *et. al*, Nucl. Instr. Meth. Phys. Res. **B248**, 7 (2006).
 - [18] S.R. Gunn, H.G. Hicks, H.B. Levy, and P.C. Stevenson, Phys. Rev. **107**, 1642 (1957)
 - [19] S.S. Kapoor, D.M. Nadkarni, R. Ramanna, and P.N. Rama Rao, Phys. Rev. **137** , B511 (1965)
 - [20] P.C. Stevenson, H.G. Hicks, J.C. Armstrong, Jr. and S.R. Gunn, Phys. Rev. **117**, 186 (1960)
 - [21] A. Tudora, G. Vladuca, and B. Morillon, Nucl. Phys. A **740**, 33 (2004)
 - [22] U. Brosa, S. Grossman and A. Muller, Phys. Rep. **197** 167 (1990)
 - [23] P.P. Dyachenko, B.D. Kuzminov, and M.Z. Tarasko, Sov. J. Nucl. Phys. **8**, 165 (1969)
 - [24] S. Grossmann, U. Brosa and A. Muller, Nucl. Phys. A **481**, 340 (1988).

TABLE I: Measured TKE release for $^{235}\text{U}(\text{n,f})$		
E_n (MeV)	\overline{TKE} (MeV)	Uncertainty (\overline{TKE}) (MeV)
3.7	167.4	0.7
4.7	165.7	0.8
5.8	167.7	0.8
7.2	166.5	0.8
9.0	166.2	0.8
11.8	165.1	0.7
16.8	163.4	0.7
24.2	162.9	0.7
34.2	161.5	0.8
45.0	162.1	0.8

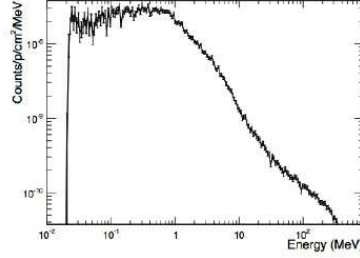


FIG. 1: The calculated neutron spectrum in the 15R beam area [11]

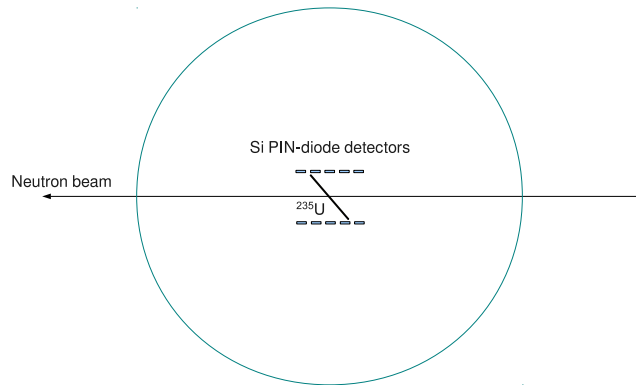


FIG. 2: (Color-online) Schematic diagram of the experimental apparatus.

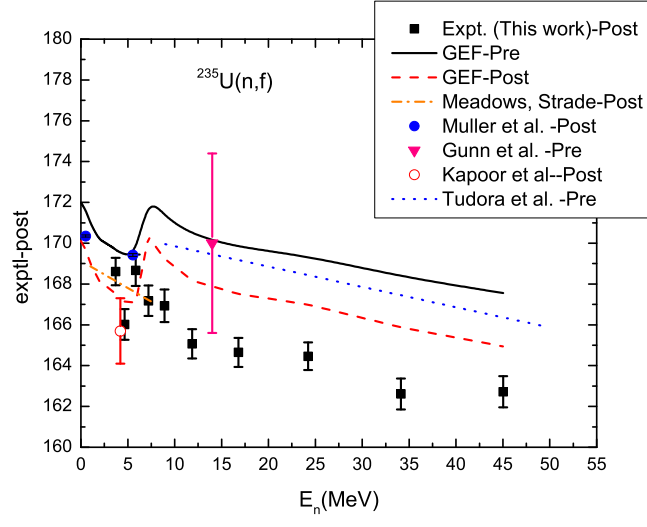


FIG. 3: (Color-online) TKE release data for $^{235}\text{U}(n,f)$

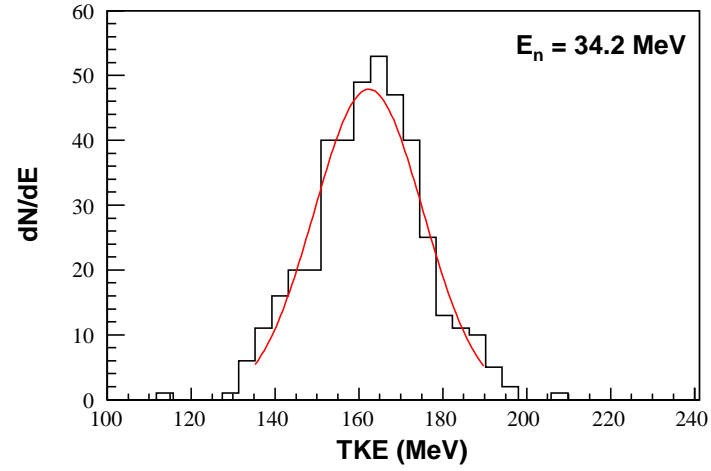
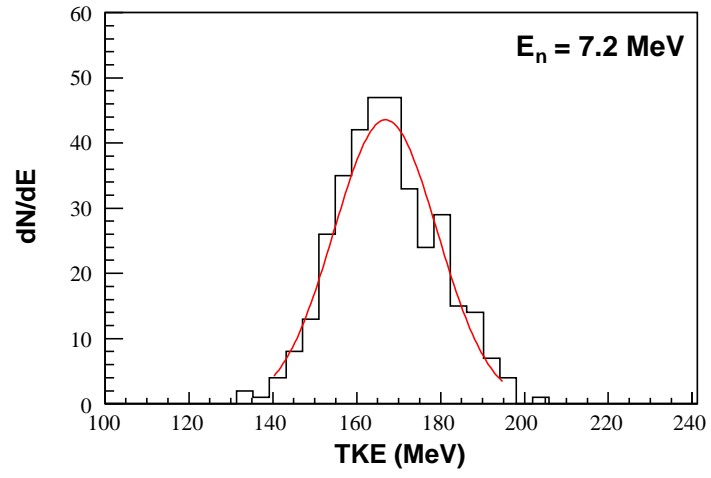
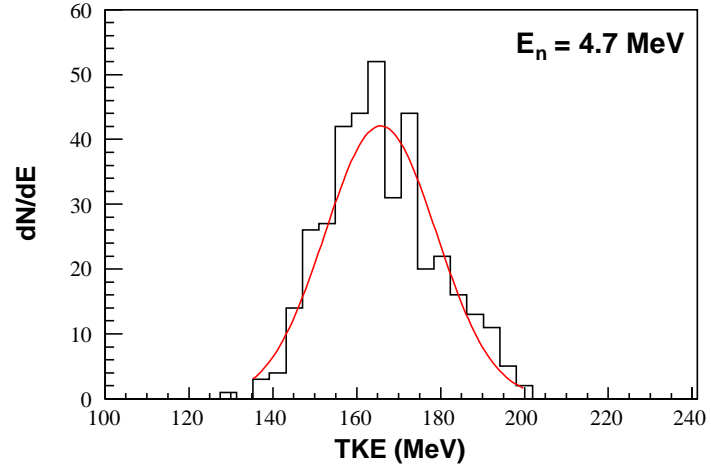


FIG. 4: (Color-online) Typical TKE distributions for $^{235}\text{U}(\text{n.f})$

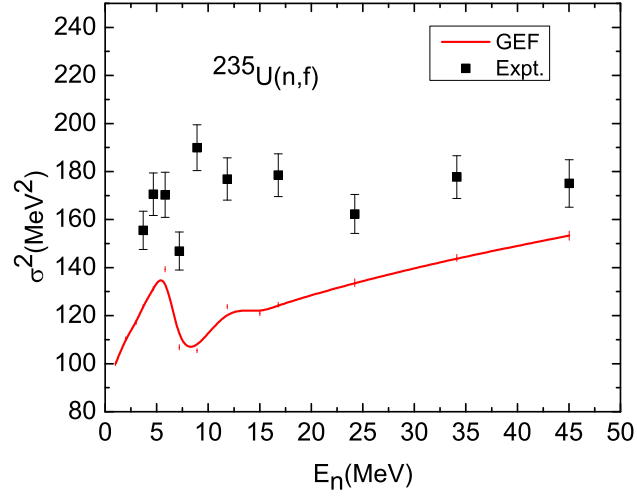


FIG. 5: (Color-online) Variance of the TKE distribution data for $^{235}\text{U}(\text{n},\text{f})$

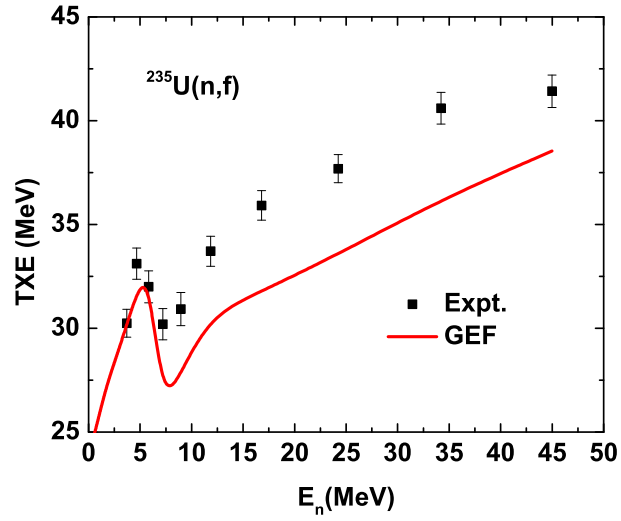


FIG. 6: (Color-online) TXE data for $^{235}\text{U}(\text{n},\text{f})$